Journal of Superconductivity and Novel Magnetism (2019) 32:1307–1317
https://doi.org/10.1007/s10948-018-4819-0

ORIGINAL PAPER

Thermophysical Investigations of Ultrasonically Assisted Magnetic Nanofluids for Heat Transfer

Prashant B. Kharat[1] · Ashok V. Humbe[1] · Jitendra S. Kounsalye[1] · K. M. Jadhav[1]

Received: 22 June 2018 / Accepted: 23 July 2018 / Published online: 6 August 2018

Abstract

The $NiFe_2O_4$ magnetic nanoparticles synthesized and used to prepare stable water-based magnetic nanofluids of various concentrations by ultrasonically assisted two-step techniques. Thermophysical investigations are made on the nanofluids at different temperatures ranging from 20 to 80 °C. The measurements revealed that the thermal conductivity of nanofluids significantly enhances with an increase in the percentage of nanoparticle volume fraction. The thermal conductivity measurements showed that the maximum enhancement is 32.65% achieved at 1% nanoparticle volume fraction and at 80 °C. Specific heat of nanofluids was decreased with increasing nanoparticle volume fractions, and it augments with increasing temperature. Viscosity measurements showed that nanofluid had a Newtonian behavior at all nanoparticle volume fractions and temperatures considered. The viscosity of the nanofluid increased with increasing nanoparticle concentration and decreasing temperature. Experimental results revealed that the viscosity sensitivity to temperature variation is minor, while it is more sensitive to the variations of nanoparticle volume fraction. The density of nanofluids was increased with increasing nanoparticle volume fractions and decreased with increasing temperature. Lastly, efforts were made to provide a precise correlation to estimate the thermal conductivity, as well as other thermophysical properties at various temperatures and volume fractions of nanoparticles. The comparison between the results and the correlation results showed a good agreement.

Keywords Nickel ferrite · Water · Nanofluids · Thermophysical · Thermal conductivity

1 Introduction

Heat transfer science is one of the most important branches in most of the applied engineering sciences in the present scenario. The good heat management is the essential need of the energy management, saving energy, and achieving a higher efficiency of the equipment and devices [1]. Since a way back, various conventional fluids such as water, ethylene glycol, oil, etc. are used in heat transfer systems [2]. The fluid heat transfer is broadly used in various industries including the cooling of power plant equipment, automobile industry, electronic equipment, and heat exchangers [3]. Improved heat transfer rate by fluids raises thermal efficiency while improving the design and performance of thermal systems. These conventional fluids in the industry have insignificant heat transfer capability [4]. From an industrial perspective, there is a need for developing fluids with a higher thermal conductivity and higher heat transfer coefficients [5]. The heat transfer coefficients of the conventional fluids can be enhanced by suspending nanoparticles in the base fluid, and the product fluid is termed as "nanofluids" [6].

Nanofluids, are a new achievement, have a higher heat transfer potential than conventional heat transfer fluids. As the heat transfer capacities of nanofluids significantly depend on the thermal conductivities of nanoparticle and base fluid, the augmentation in thermal conductivity values of metallic nanofluids is reported to be significant [7]. Typically, conventional fluids such as water, oil, and ethylene glycol have low heat transfer capacities than metal nanoparticles such as Ag, Cu, CuO, Al_2O_3, Fe_2O_3, SiO_2, TiO_2, etc. with a notable thermal conductivity [8]. Nanofluids with nanoparticles have many applications in bioengineering, aerospace, microfluidics, mechanical engineering, chemical engineering, electronic packing, and renewable

✉ Prashant B. Kharat
pbk9403750321@gmail.com

✉ K. M. Jadhav
drjadhavkm@gmail.com

[1] Department of Physics, Dr. Babasaheb Ambedkar Marathwada University, Aurangabad, Maharashtra, 431001 India

energy systems [9, 10]. Among the existing nanoparticles, magnetic nanoparticles (such as $CoFe_2O_4$, $NiFe_2O_4$, $MnZnFe_2O_4$, $MnFe_2O_4$, Fe_2O_3, Fe_3O_4, Co, and Fe) have attracted special attention due to their remarkable features [11–15]. Due to the very small size of the particles, corrosion, impurities, and pressure drop are reduced significantly. Furthermore, the stability of nanofluids is considerably improved against sedimentation. By adding nanoparticles to the base fluid in a nanofluid, thermophysical properties will change relative to the base fluid. Since thermophysical properties are dependent on temperature and the concentration of nanoparticles in the base fluid, maximum desirable thermophysical properties can be achieved by changing these two factors (temperature and concentration) [16, 17]. Generally, nanofluids have a high thermal conductivity most important to a high heat transfer rate. The thermal conductivity of nanofluids plays a very important role in heat transfer applications [18]. The thermal conductivity of nanoparticles is much higher than that of liquids. Consequently, the addition of nanoparticles to liquids will increase their thermal conductivity [19]. Thermal conductivity enhancements in nanofluids are generally described using the effective medium theory (EMT) that is based on Maxwell's mean field theory [20]. There are reports in the literature showing thermal conductivity enhancement in nanofluids to be within [21] or beyond [19] the estimates of effective medium theory.

A short literature review based on previous reports of the improved thermophysical properties of nickel ferrite ($NiFe_2O_4$) and water-based nanofluids is presented below. Karimi et al. studied the thermal conductivity of magnetic nanofluids containing MFe_2O_4 (M = Fe and Co) nanoparticles suspended in deionized water in the volume fractions between 0 and 4.8%. The experimental results show that the thermal conductivity of MNFs increases with increase in volume fraction [22]. In his other investigation, the thermal conductivity of $NiFe_2O_4$ nanoparticles dispersed in deionized water in concentrations between 0 and 2% and in the temperature range of 25–55 °C. The maximum enhancement in thermal conductivity of nanofluids is 17.2% at 2% volume concentration and in temperature of 55 °C [23]. Amani et al. studied $MnFe_2O_4$/water nanofluid in 0.25 to 3% concentrations. The thermal conductivity of nanofluid enhanced with increasing of nanoparticle volume fraction and increasing temperature. The highest thermal conductivity improvement is achieved by 26.4% at 60 °C and 3 vol.% of nanoparticle concentration [24]. Shahsavar et al. conducted studies of the thermal conductivity and viscosity of the water-based hybrid nanofluid containing both Fe_3O_4 magnetic nanoparticles, and carbon nanotubes (CNTs) are measured at temperatures between 25 and 55 °C, Fe_3O_4 volume concentrations between 0.1 and 0.9%, and CNT volume concentrations between 0 and 1.35% [25].

Therefore, in the present work, a systematic experimental study on the thermophysical response of $NiFe_2O_4$–water nanofluids to the heat transfer are made for the basic understanding of how the $NiFe_2O_4$ nanoparticles behave in water and how they interact with each other and also with the molecules of water. Preparing the stable and homogeneous suspensions of $NiFe_2O_4$ nanoparticles in water and attaining a deeper understanding of particle–fluid interactions as functions of concentration and temperature are the main concern of the present work. In this work, the synthesis, heat transfer characteristics, and the thermophysical properties of $NiFe_2O_4$–water nanofluids are studied experimentally; validation with current theoretical models indicates that interface in this nanofluid system prevents the use of simple models. For systems such as this likely due to the presence of $NiFe_2O_4$ and associated thermal resistance may need to be better modeled. Our studies clearly point to the need for this. In addition, the paper is intended to formulate a relationship between thermophysical properties and concentration of $NiFe_2O_4$ in nanofluids, which would be of great importance in view of the difficulties in the experimental determination of thermal conductivities of nanofluids.

2 Experimental

2.1 Materials

For the synthesis of nickel ferrite nanoparticles, primary chemicals including nickel(II) nitrate hexahydrate ($Ni(NO_3)_2*6H_2O$)), iron(III) nitrate nonahydrate ($Fe(NO_3)_3*9H_2O$)), sodium hydroxide (NaOH), acetone (CH_3COCH_3), Di water (H_2O), and nitric acid 69% (HNO_3) were used without any purification. Chemicals were of analytical regent (AR) grade and purchased from Merck Millipore.

2.2 Synthesis of $NiFe_2O_4$ and Preparation of Nanofluids

Aqueous solutions of nickel nitrate and ferric nitrate were prepared separately in stoichiometric ratio of 1:2 to obtain the precursors. Both the solutions were mixed together and stirred for 1 h to get a homogeneous mixture. pH of the mixture was found to be 3. Then, 2 M NaOH solution was added drop by drop to the above mixture with simultaneous stirring until the pH reaches 9. A brown precipitate thus obtained was heated at boiling temperature for 2 h, was allowed to cool, and washed several times with distilled water to remove impurities. Then, 200 ml of 2 M aqueous HNO_3 solution was added to the above precipitate and stirred for 1 h. The supernatant solution was removed, and the residue was cleaned thrice with acetone. These

nickel ferrite nanoparticles were dried overnight at the 60 °C in a microwave furnace. Nickel ferrite nanofluids of various concentrations (0.2, 0.4, 0.6, 0.8, and 1% by volume) were prepared by dispersing appropriate amount of nanoparticles in water by employing ultrasonication for 3 h to get a homogenous suspension without any phase separation and sedimentation. The detailed flowchart and procedure of preparation of nanofluid are given in our earlier reports [26, 27].

2.3 Characterizations

2.3.1 Properties of $NiFe_2O_4$ Nanoparticles

The structural, morphological, elemental, and magnetic analysis of prepared nickel ferrite magnetic nanoparticles were studied using X-ray diffractometer (XRD), field emission scanning electron microscope (FESEM), energy dispersive X-ray spectroscopy (EDS), and vibrating sample magnetometer (VSM). The XRD pattern was compared with the Joint Committee on Powder Diffraction Standards (JCPDS) (card number 10-0325). XRD (BRUKER D8 Advance) with Cu-Kα radiation ($\lambda = 1.5418$ Å) in the 2θ ranging from 20° to 80° was used for phase identification and crystal structure analysis of the $NiFe_2O_4$ magnetic nanoparticles. Based on the Debye–Scherrer equation, from the full width at half maximum (FWHM) of the highest-intensity diffraction peak (311), the crystallite size was calculated. The morphology and particle size distribution of the $NiFe_2O_4$ nanoparticles were determined by FESEM micrographs. The compositional and elemental percentage were resolute from the EDS spectrum of the $NiFe_2O_4$. The magnetic properties including saturation magnetization (M_s), remanence magnetization (M_R), and coercivity (H_c) of the $NiFe_2O_4$ were analyzed from M–H plot obtained from VSM.

2.3.2 Thermophysical Properties

The thermophysical properties of $NiFe_2O_4$–water nanofluids were analyzed using thermal conductivity meter, differential scanning calorimeter, viscometer, and density meter. The thermal conductivity of the prepared nanofluids was measured from KD2 Pro (Decagon Devices, Inc., USA) thermal property analyzer with a maximum error of about 5%. The transient hot wire (THW) technique was employed in KD2 Pro for measurement of thermal conductivity. A sample container of the cylindrical testing chamber with a diameter of 30 mm and length of 100 mm and the KD2 Pro KS-1 (stainless steel single needle) sensor with a length of 60 mm and a diameter of 1.27 mm vertically inserted into the center of nanofluids were used. Each measurement cycle was 60 s. Heat is applied for 30 s. Thirty seconds were allowed for temperature equilibration before heating starts. Each measurement cycle was of 60 s. The thermal conductivity (k) of nanofluids was obtained by the following equation:

$$k = \frac{q(\ln t_2 - \ln t_1)}{4(\Delta T_2 - \Delta T_1)} \quad (1)$$

where q is the constant heat rate and T_2 and T_1 are the changes in temperature at times t_2 and t_1, respectively. DSC-60 (Shimadzu Corporation) Plus Series Differential Scanning Calorimeter were used to record for the specific heat of the nanofluids. The Anton-Paar portable density meter was used for the measurement of the density of nanofluids. The viscosities of the nanofluids were recorded by the Brookfield DV-III viscometer. The stable temperature bath was used to stabilize the temperature of the samples. The measurements were carried out three times, and the average values of the carried out measurement were recorded for all the thermophysical measurements.

3 Results and Discussion

3.1 Structural, Morphological, and Elemental Analysis

The recorded XRD pattern of the prepared spinel $NiFe_2O_4$ nanoparticles is shown in Fig. 1. The figure shows that the prepared nanoparticles have a well crystalline phase. Oxygen position and octahedral (B) and tetrahedral (A) positions of ions are shown in the inset of Fig. 1. The crystal planes of (220), (311), (222), (400), (422), (333), (440), (531), (620), (553), and (444) were observed in XRD; it was also compared with the Joint Committee on Powder Diffraction Standards (JCPDS) (card number 10-0325) [28]. The XRD data reveals that the sample was crystallized in single phase spinel structure corresponding to the Fd3m space group [29, 30]. The calculated structural parameters [31, 32] are listed in Table 1.

The FESEM micrographs of $NiFe_2O_4$ are shown in Fig. 2a, b. The FESEM micrographs show that the prepared particles are spherical in nature, and the grains are distributed homogeneously. The nanoparticles are of the nanocrystalline nature, and grains are agglomerated; this agglomeration is attributed to high surface energy and magnetic interactions of the $NiFe_2O_4$ magnetic nanoparticles [33]. Thus, agglomeration and some of the elongated particles are observed in FESEM micrographs. Similar observations were reported for nanocrystalline mixed spinel ferrite prepared using the wet chemical route [34]. Obtained data from FESEM micrographs, i.e., average particle size (D') and specific surface area (SSA) are listed in Table 1.

The size distribution was obtained from the particle size distribution histogram, and for that, we have measured

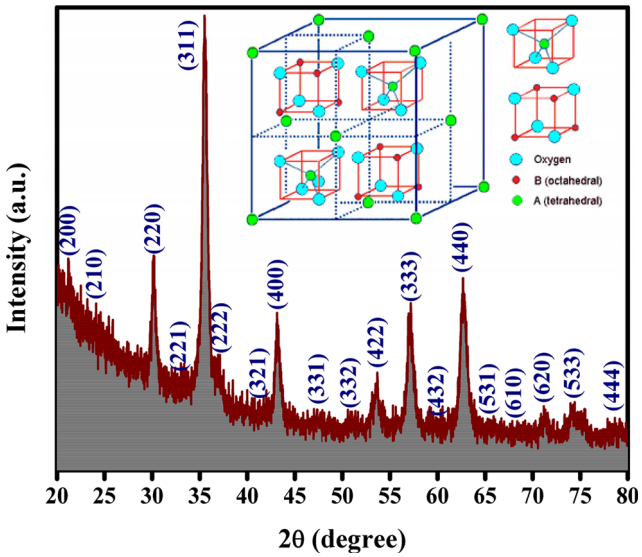

Fig. 1 X-ray diffraction of the nickel ferrite nanoparticles; inset, spinel structure

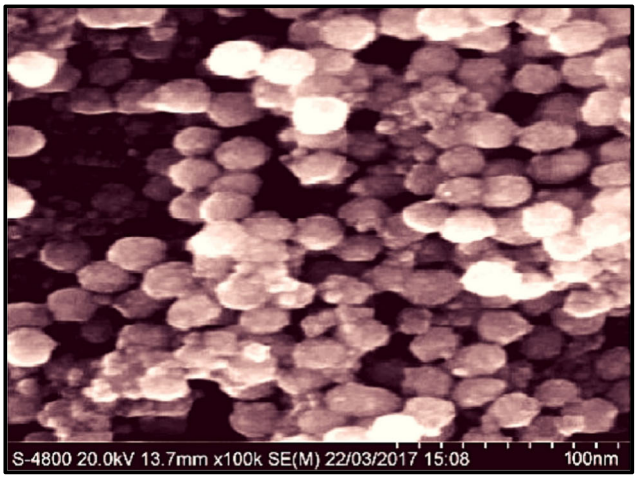

(a)

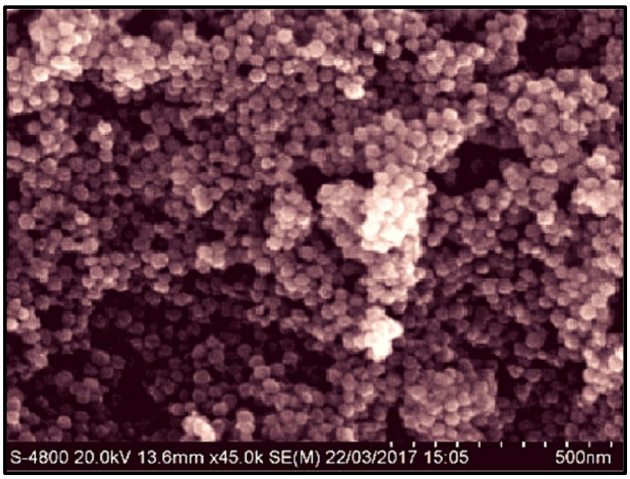

(b)

Fig. 2 **a**, **b** FESEM micrograph of the nickel ferrite nanoparticles

the average size of 300 particles observed in the FESEM micrograph. The size distribution histogram of the $NiFe_2O_4$ magnetic nanoparticles is shown in Fig. 3. The average particle size obtained from the micrograph is (D'), which is smaller than earlier reports on $NiFe_2O_4$ nanoparticles prepared by co-precipitation method [35]. The observations obtained from the FESEM micrographs are in good agreement in XRD pattern.

The observed elemental spectrum of $NiFe_2O_4$ magnetic nanoparticles is shown in Fig. 4. The elemental spectra show that all the peaks belong to the present elements in the composition of $NiFe_2O_4$, i.e., nickel (Ni), iron (Fe), and oxygen (O). The percentage of Ni, Fe, and O is shown in the inset of Fig. 4. The elemental spectrum of $NiFe_2O_4$ magnetic nanoparticles reveals the composition has prepared without any impurity. The obtained atomic ratio of Ni, Fe, and O match well with that expected and maintains the stoichiometric proportion. This shows the significance of the co-precipitation technique for the synthesis of the nanocrystalline $NiFe_2O_4$ magnetic nanoparticles.

3.2 Magnetic Analysis

The M–H hysteresis plot of the $NiFe_2O_4$ magnetic nanoparticles at the 300K temperature is shown in Fig. 5. From the hysteresis plot, the magnetic parameters reveal that the M_s, M_R, and H_c are also measured, and it is found to be 81.91 emu/g, 2.35 emu/g, and 39.68 Oe, respectively. The sample has high M_s and tiny M_R and H_c, which shows the sample exhibits a superparamagnetic nature [36]. The prepared magnetic nanoparticles have superior magnetization as compared with an earlier report on $NiFe_2O_4$ prepared by sol-gel [34] and chemical co-precipitation [37] method. The magnetic behavior of present $NiFe_2O_4$ nanoparticles can be explained by Neel's ferrimagnetism model [33]. Using Neel's model, the theoretical magneton number of $NiFe_2O_4$ nanoparticles was calculated as

$$\eta_B = M_B - M_A \tag{2}$$

Table 1 Molecular weight (M_w), lattice constant (a), crystallite size (D), particle size (D'), specific surface area (SSA), X-ray density (ρ_{XRD}), bulk density (ρ_{BULK}), and porosity (Pt) of oleic acid-coated nickel ferrite nanoparticles

Sample	M_w (g/mol)	a (Å)	D (nm)	D' (nm)	SSA (m^2/g)	ρ_{XRD} (g/cm^3)	ρ_{BULK} (g/cm^3)	Pt (%)
$NiFe_2O_4$	234.38	8.355	10.40	9.5 ± 2	115.94	5.336	3.633	31.83

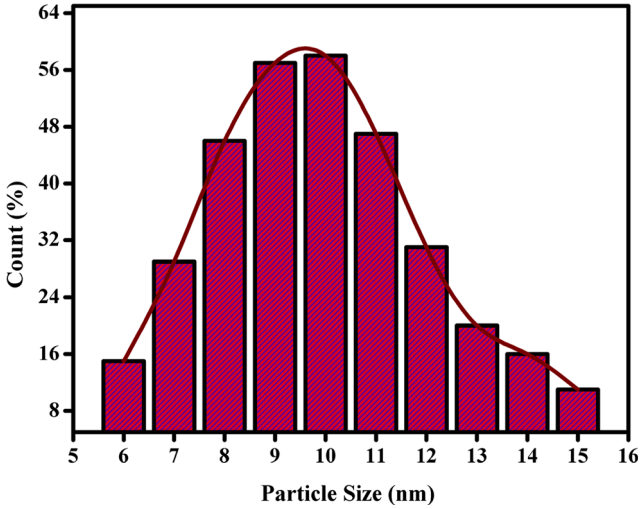

Fig. 3 Histogram showing particle size distribution from FESEM micrograph of the nickel ferrite nanoparticles

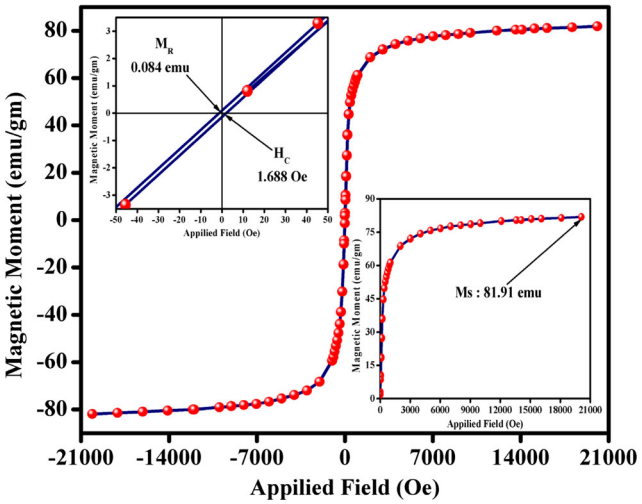

Fig. 5 M–H hysteresis curve of the nickel ferrite nanoparticles

where M_B and M_A are the magnetic moments of octahedral and tetrahedral sites, respectively. It is a well-known fact that the Ni^{2+} has a preference for octahedral B sites, and Fe^{3+} occupies each tetrahedral site as well as the octahedral site. However, Ni^{2+} ions have octahedral site preference and must occupy tetrahedral A sites. The resulting cation distribution can be written as $(Ni_{0.347}Fe_{0.653})^A$ and $(Ni_{0.653}Fe_{1.347})^B$. Thus, the Ni^{2+} ion distribution over both sublattices must be well supported and confirmed.

The magnetic properties of nanoparticles are different which are found in the bulk materials. Magnetic domains are the bunch small regions that exist in the magnetic materials. These magnetic domains are caused by the equilibrium of numerous energy footings, the exchange energy, the magneto-crystalline anisotropy, and the magnetostatic energy [38]. Due to the exchange energy available in magnetic materials, they start to align with the magnetic moment with the similar direction, and the magneto-crystalline anisotropy changes show turning in a magnetic moment in the same direction. But the magneto-static energy is responsible for the disappearance of the magnetization in the magnetic materials [39]. The magnetization that appears in the magnetic materials is the sum of the total magnetization associated with all domains present. It discovered that the magnetic domains in the ferromagnetic crystals have the smallest size (below 50 nm) whereby the ferromagnetic material cannot divide further into another small domain and are termed as single or monodomain particles [40]. Thermal energy acts as the main part in the magnetic uncertainty of single-domain magnetic particles. Due to the small particle size obtained in preparing the $NiFe_2O_4$ nanoparticles, it is clear that the size of the nanoparticles were below the critical size, showing that the prepared sample may have a single magnetic domain. Figure 6 shows that the particle size and coercivity depended on the magnetic domain curve.

It is clearly revealed by FESEM (Fig. 2a, b) micrographs that the prepared $NiFe_2O_4$ are at average particle size of 9.5 nm. Hence, the prepared $NiFe_2O_4$ nanoparticles exhibit a superparamagnetic nature. Every nanoparticle of the

Fig. 4 EDS spectrum of the nickel ferrite nanoparticles

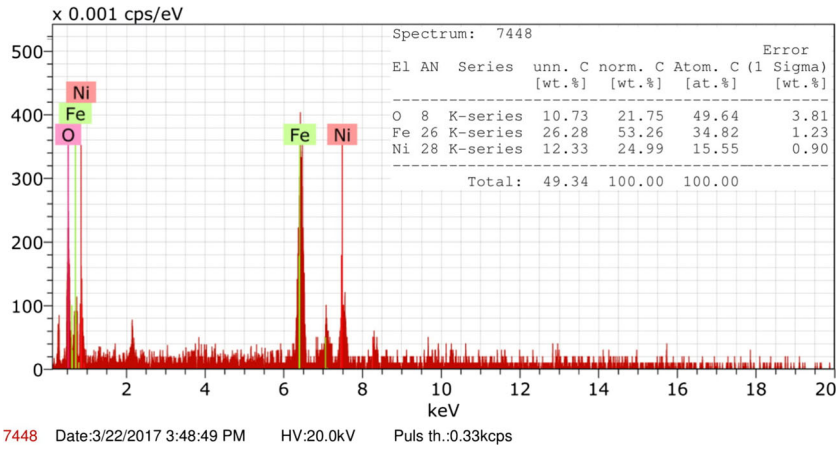

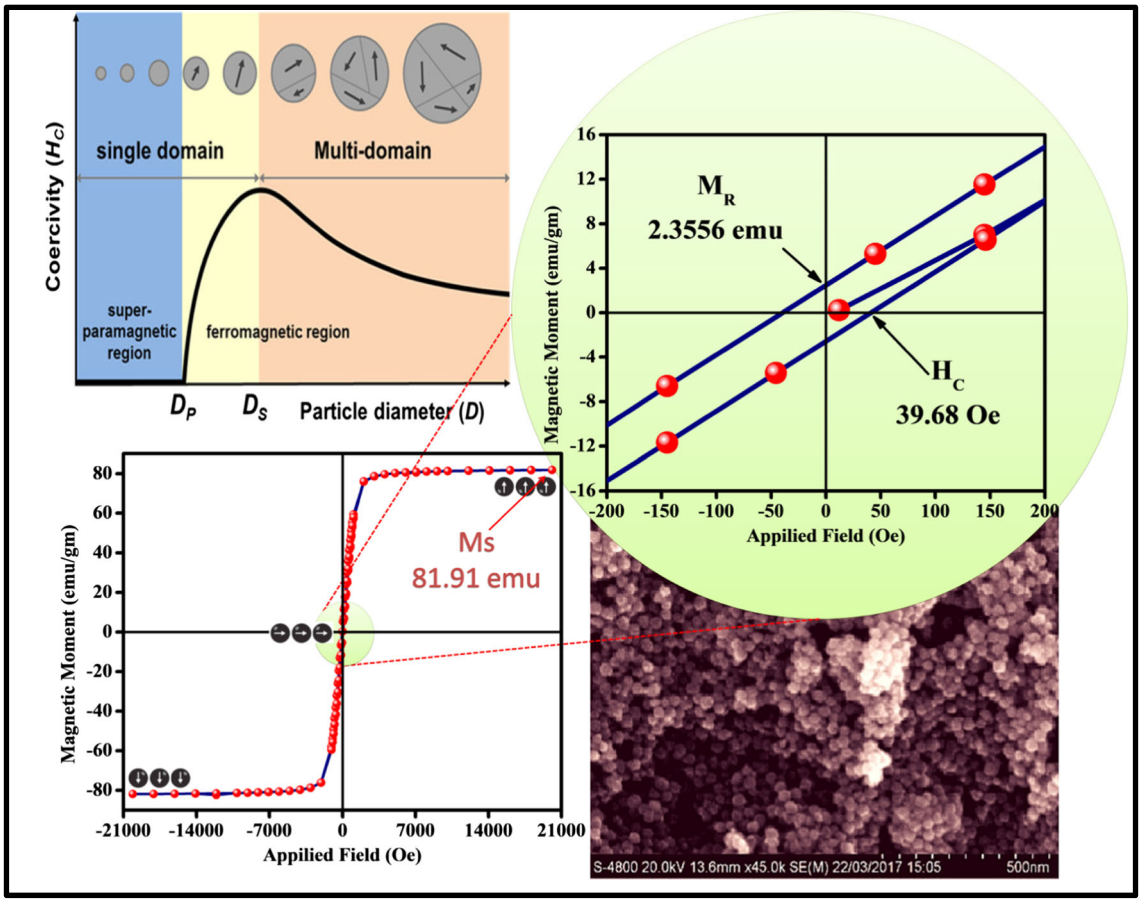

Fig. 6 Particle size and coercivity depended on magnetic domain curve

prepared $NiFe_2O_4$ exhibits a high magnetic moment, and the magnetic domains change its alignments continuously, due to its superparamagnetic nature. A superparamagnetic material exhibits a very quick response to the applied magnetic field. Therefore, in the superparamagnetic state, the $NiFe_2O_4$ nanoparticle acts as a paramagnetic atom with a giant spin [41].

3.3 Thermophysical Analysis of Nanofluids

The addition of nanoparticles in the host liquid is significantly affected by its thermophysical properties such as thermal conductivity, density, viscosity, and specific heat that affect the convective heat transfer. For the high performance of the cooling systems, the heat transfer fluid should have excellent thermophysical properties [42]. The nanoparticles are playing a vital role and drastically enhance the thermophysical properties of the host liquid. Figure 7 illustrates these thermophysical properties. Different nanomaterials changed their parameters to a different extent. The concentration of nanoparticles, purity level, shape, and size of nanomaterials are some of the prime factors that significantly alter the thermophysical properties [18].

3.3.1 Thermal Conductivity

The changes in the thermal conductivity of the nanofluids change with volume fraction as shown in Fig. 8. From the observation, it is revealed that the thermal conductivity of the $NiFe_2O_4$–water nanofluids is augmented with increasing nanoparticle volume fraction from 0.2 to 1%. The similar augmentation trend is observed for the entire volume fraction. In the present work, the thermal conductivity of $NiFe_2O_4$ nanoparticles is 4.8 W/mK, while it is approximately 0.6 W/mK for water. Hence, adding the $NiFe_2O_4$ nanoparticles into water would enhance its thermal conductivity. In fact, the higher nanoparticle volume fraction in the nanofluid leads to a smaller distance between the nanoparticles; consequently, the probability of formation of clusters due to van der Waals attraction increases [26]. There are various other reasons for thermal conductivity augmentation of water in the presence of nanoparticles such as the Brownian motion of nanoparticles, the creation of complexes of nanoparticles and collisions between them, the formation of a layer of fluid molecules together with the surfaces of the nanoparticles, and clustering of nanoparticles [24, 43]. Clustering of nanoparticles leads in the creation of paths with

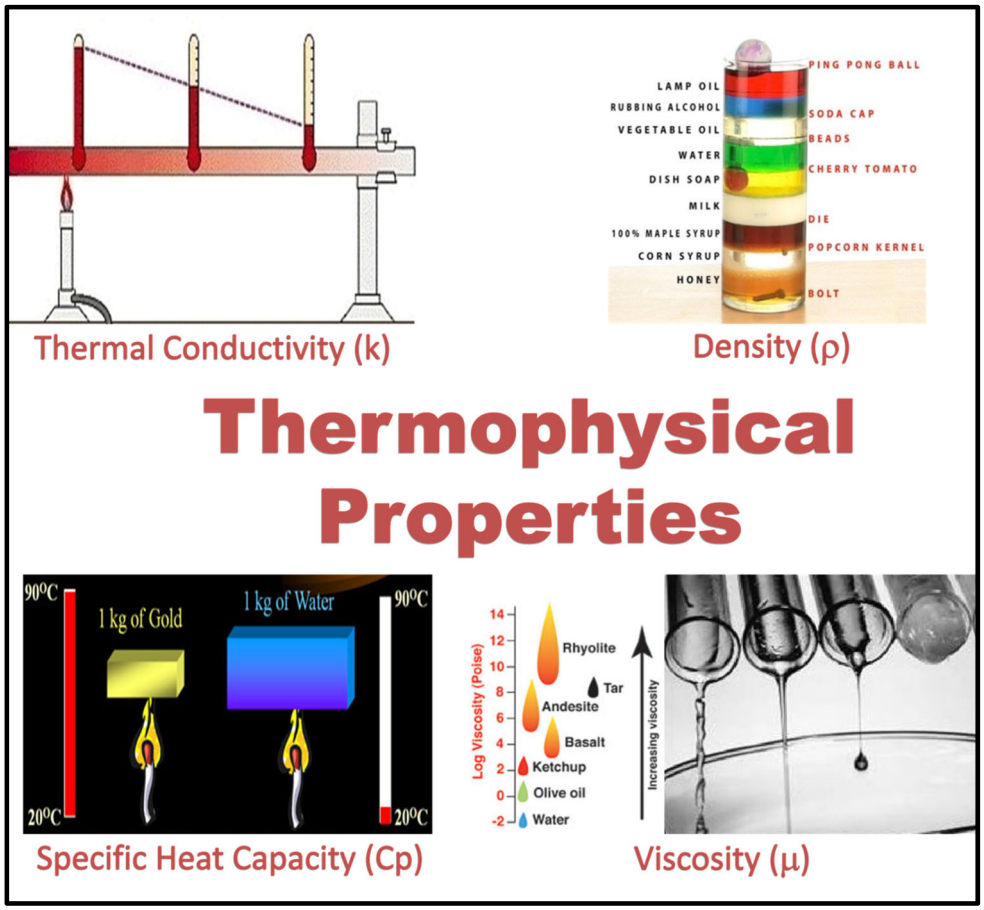

Fig. 7 Illustration of thermophysical properties: thermal conductivity, density, specific heat capacity, and viscosity

lower thermal resistance, which would enhance heat transfer in the fluid [18]. This phenomenon can influence the thermal conductivity of nanofluids.

The effect of temperature on the thermal conductivity of the nanofluids is also shown in Fig. 8. The experimental results show the enhancement in the thermal conductivity of the nanofluids with increasing the temperature from 20 to 80 °C. The main reason for thermal conductivity enhancment due to the temperature increase can be characterized by Brownian motion and the increase in interactions between the nanoparticles [44]. However, the thermal conductivity of water considerably augments with increasing temperature, while the thermal conductivity of nanofluid slightly enhances. In fact, when nanoparticles are present in the water, the creation of nanoclusters takes place. Therefore, the Brownian motion is limited due to van der Waals forces; as a result, the effect of temperature becomes lower [26]. The thermal conductivity measurements show that the maximum enhancement of thermal conductivity of nanofluid is 32.65%, which occurs in a nanoparticles volume fraction of 1% and temperature of 80 °C.

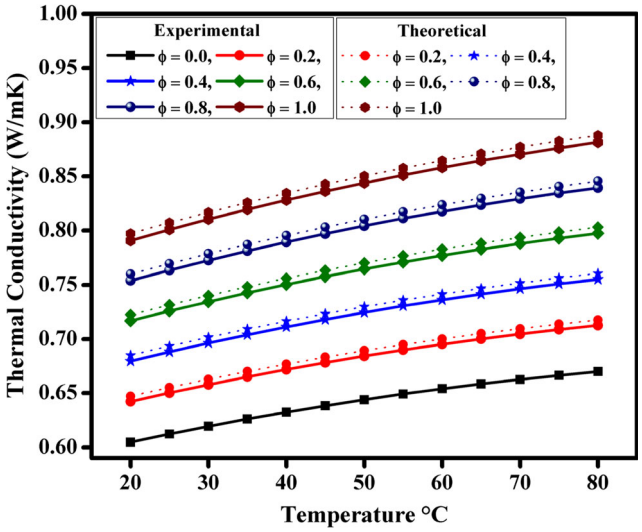

Fig. 8 Variation in thermal conductivity of $NiFe_2O_4$–water nanofluids with temperature and volume fraction

The observed thermal conductivity also tried to estimate the mathematical model shown in Fig. 8 (dotted lines). The thermal conductivity is estimated by the equation,

$$\frac{k_{nf}}{k_f} = \frac{k_p + 2k_f + 2\varphi(k_p + k_f)}{k_p + 2k_f + \varphi(k_p + k_f)} \quad (3)$$

where the thermal conductivity of the nanofluid k_{nf}, k_f is the thermal conductivity of the base fluid and φ is the volume fraction of the particles.

The estimated values have a very tiny difference, and the theoretical curve flows to the experimental curve for nanoparticle volume fraction from 0.2 to 1%. This shows that the mathematical model used here is most suitable for estimating the thermal conductivity of the $NiFe_2O_4$–water nanofluids.

3.3.2 Specific Heat

The specific heat is the energy required to heat the sample by 1 °C, which is the specific heat capacity of the nanofluid sample, and this has a significance in the heat transfer systems. The effect of the addition of the $NiFe_2O_4$ nanoparticles is shown in Fig. 9. From the experimental data, it can be seen that the specific heat of the nanofluids is decreased with increasing nanoparticle volume fraction from 0.2 to 1%. Here, the lower specific heat of nanoparticles in the base fluid results in a decrease in the specific heat capacity of the nanofluid with an increase in particle concentration. Effect of the temperature is also revealed in Fig. 9. The nanofluids were studied in the temperature range of 20 to 80 °C, and the observations show that there are very small changes in the specific heat of the nanofluids with increasing temperature.

Further, the estimated specific heat (C_{nf}) of a nanofluid with the experimental values are presented in Fig. 9 and that is straightforward and estimated based on the physical principle of the mixture rule [45] as,

$$C_{nf} = \frac{\varphi\rho_p C_p + (1-\varphi)\rho_f C_f}{\varphi\rho_p + (1-\varphi)\rho_f} \tag{4}$$

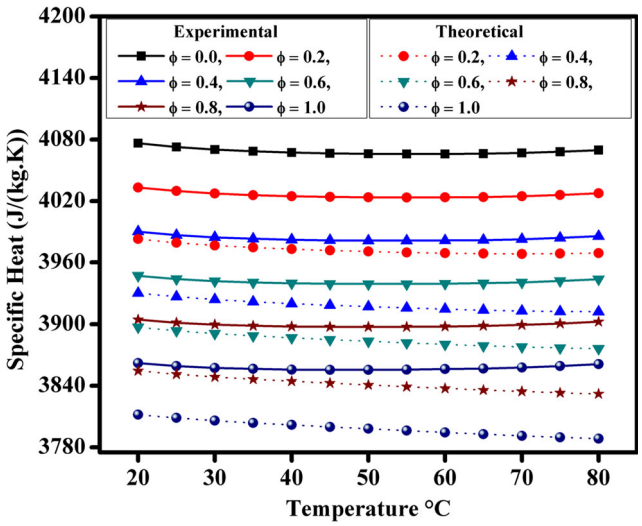

Fig. 9 Variation in specific heat of $NiFe_2O_4$–water nanofluids with temperature and volume fraction

where ρ_p is the density of nanoparticles, C_p is the specific heat of nanoparticles, ρ_f is density heat of base liquid, C_f is specific heat of base liquid, and φ is volume fraction.

The experimental values obtained are rationalized with the theoretical values, and it is found that there is an average of 1.50% deviation in the experimental and theoretical values. This deviation in the observed values regarding calculated results is likely due to the formation of nanolayer between the particle and the fluid. The surface of the nanoparticles is multiple phases. Hence, specific heat capacity, which is a thermophysical quantity, is dependent on not only the bulk phases but also the nature of interfacial nanolayers. Hence, relevant corrections are needed to account for the observed behavior [45].

3.3.3 Viscosity

The viscosity of the heat transfer fluids (nanofluids) is a very important propert; it is directly related to the energy consumptions of the heat transfer system. The higher the viscosity, the more energy will be required to circulate the nanofluid in the system [27]. The effect of nanoparticle volume fraction in the nanofluids is plotted in Fig. 10. The observed results reveal that the viscosity increases with increasing nanoparticle volume fraction from 0.2 to 1%. The viscosity effect is to withstand the relative movement of the liquid. In fact, it plays a key role in the momentum transfer between the layers of liquid, which acts long as there are movements between the layers. This phenomenon is because of the van der Waals forces between the molecules. Therefore, the dispersion of nanoparticles in water would increase its viscosity as a result of the interactions between them. By increasing the number of nanoparticles in a specific amount of water, larger nanoclusters arise due to the van der Waals forces between them, which can prevent the movement of water layers on each other. It may lead to improvement in viscosity of nanofluids [46, 47].

Figure 10 also reveals that the viscosity of the nanofluid reduces with an increase in temperature. This is due to the fact that, with enhancing temperature, the intermolecular interactions between the molecules become feeble and thus the viscosity is reduced. While optimizing nanofluids, it is important to assure that these nanofluids exhibit a Newtonian behavior without increasing the need for extra pumping power [48]. Primarily, temperature and particle volume fraction influence the viscosity of nanofluid. The effective viscosity (μ_{nf}) of a suspension of solids may be estimated as:

$$\frac{\mu_{nf}}{\mu_f} = 1 + 2.5\,\varphi \tag{5}$$

Here, φ is the volume fraction of the particle and μ_f is the viscosity of the base fluid under consideration. The

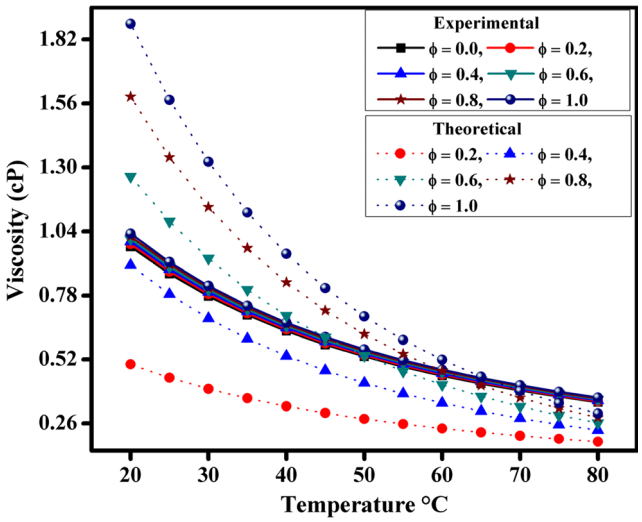

Fig. 10 Variation in viscosity of $NiFe_2O_4$–water nanofluids with temperature and volume fraction

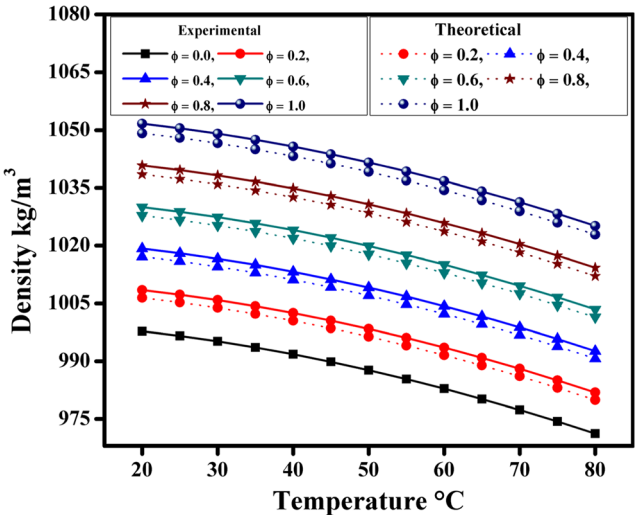

Fig. 11 Variation in the density of $NiFe_2O_4$–water nanofluids with temperature and volume fraction

experimental and theoretical results show much difference between 20 and 50 °C. It is essential to note that this model does not estimate the effective viscosity of nanofluids up to 55 °C temperature reported here reliably. Further, the experimental and theoretical results show good agreement from 55 to 80 °C. Therefore, the pressure drop problems related with the flow of nanoparticle inside the thermal systems cannot be ignored and is a limitation of the nanofluid reported here.

3.3.4 Density

The physical properties of the heat transfer system which are the friction factor, pump loss, and Reynolds number significantly depend on the density of the heat transfer fluids (nanofluids). The density of any nanofluid is directly related to particle volume fraction. The density of the nanofluids rises approximately in a linear manner with increasing volume fraction from 0.2 to 1%. Density decreases with increase in temperature of the fluid.

The theoretical model accounts for the variation in concentration at various temperatures [49]. In order to determine the rheology of suspensions, volume concentration is often used instead of mass concentration. Once the volume concentration is determined, the density of the nanofluid can be determined from,

$$\rho_{nf} = \varphi_p \rho_p + (1 - \varphi)\rho_f \tag{6}$$

where ρ_p is the density of particles, ρ_f is the density of the base liquid, and φ_p is the volume fraction of the particles

Experimental and theoretical studies (Fig. 11) show the decrease in density as a function of temperature. This decrease in density is mainly due to the weakening of bonds at elevated temperatures. It can be seen that the densities obtained are well within the range. This is because density is a purely physical parameter and the interface does not play a significant role in affecting the density of the system [50]. It notes that the experimental curves follow theoretical curves for 0.2 and 1.0 volume fraction with an average 0.5% difference.

4 Conclusion

Stable $NiFe_2O_4$–water nanofluids of various concentrations of 0.0, 0.2, 0.4, 0.6, 0.8, and 1.0% have been synthesized. The thermophysical properties were studied at temperatures ranging from 20 to 80 °C. Experimental results indicated that the thermal conductivity significantly augments with an increase in the percentage of nanoparticle volume fraction. Moreover, the thermal conductivity ratio of pure water is considerably augmented with increasing temperature, while the thermal conductivity of nanofluid is slightly less enhanced. The thermal conductivity measurements showed that the maximum augmentation of thermal conductivity of nanofluids was 32.65% achieved at nanoparticles volume fraction of 1% and at 80 °C. Specific heat of nanofluids was decreased with increasing nanoparticle volume fractions and is augmented with increasing temperature. Viscosity measurements showed that all samples of the nanofluid had Newtonian behavior. Experiments also indicated that the viscosity of the nanofluid increased with increasing nanoparticle concentration and decreasing temperature. Performing the sensitivity analysis at various temperatures showed that the viscosity sensitivity to temperature variation is minor. The density of nanofluids was increased with increasing nanoparticle volume fractions and decreased with increasing temperature. Using experimental results, in

order to predict the thermal conductivity of $NiFe_2O_4$–water nanofluids, a correlation has been proposed. Comparison between experimental results and the correlated output demonstrated that the correlation has a high accuracy. Hence, this correlation can estimate the thermophysical properties of $NiFe_2O_4$–water nanofluids

Acknowledgments The authors are thankful to Professor John Philip, Indira Gandhi Center for Atomic Research Center, Kalpakkam, Tamilnadu, as well as Professor J. B. Naik, Head, University Institute of Chemical Technology, North Maharashtra University, Jalgaon, Maharashtra, and Tata Institute of Fundamental Research, Mumbai for providing thermal conductivity and specific heat, and VSM measurement facilities.

References

1. Farret, F.A., Simões, M.G.: Integration of Renewable Sources of Energy. Wiley, New York (2017)
2. Sidik, N.A.C., Jamil, M.M., Japar, W.M.A.A., Adamu, I.M.: A review on preparation methods, stability and applications of hybrid nanofluids. Renew. Sustain. Energy Rev. **80**, 1112–1122 (2017)
3. Ganvir, R., Walke, P., Kriplani, V.: Heat transfer characteristics in nanofluid—a review. Renew. Sustain. Energy Rev. **75**, 451–460 (2017)
4. Kakavandi, A., Akbari, M.: Experimental investigation of thermal conductivity of nanofluids containing of hybrid nanoparticles suspended in binary base fluids and propose a new correlation. Int. J. Heat Mass Transf. **124**, 742–751 (2018)
5. Wadekar, V.V.: Ionic liquids as heat transfer fluids–an assessment using industrial exchanger geometries. Appl. Therm. Eng. **111**, 1581–1587 (2017)
6. Das, S.K., Choi, S.U., Yu, W., Pradeep, T.: Nanofluids: Science and Technology. Wiley, New York (2007)
7. Sundar, L.S., Sharma, K., Singh, M.K., Sousa, A.: Hybrid nanofluids preparation, thermal properties, heat transfer and friction factor—a review. Renew. Sustain. Energy Rev. **68**, 185–198 (2017)
8. Gupta, M., Singh, V., Kumar, S., Kumar, S., Dilbaghi, N., Said, Z.: Up to date review on the synthesis and thermophysical properties of hybrid nanofluids. J. Clean. Prod. **190**, 169–192 (2018)
9. Amani, M., Amani, P., Kasaeian, A., Mahian, O., Pop, I., Wongwises, S.: Modeling and optimization of thermal conductivity and viscosity of $MnFe_2O_4$ nanofluid under magnetic field using an ANN. Sci. Rep. **7**, 17369 (2017)
10. Chavan, A.R., Chilwar, R.R., Kharat, P.B., Jadhav, K.: Effect of annealing temperature on structural, morphological, optical and magnetic properties of $NiFe_2O_4$ thin films. J. Supercond. Nov. Magn. 1–10. https://doi.org/10.1007/s10948-018-4565-3 (2018)
11. Sanna Angotzi, M., Musinu, A., Mameli, V., Ardu, A., Cara, C., Niznansky, D., Xin, H.L., Cannas, C.: Spinel ferrite core–shell nanostructures by a versatile solvothermal seed-mediated growth approach and study of their nanointerfaces. ACS Nan **11**, 7889–7900 (2017)
12. Wei, C., Feng, Z., Baisariyev, M., Yu, L., Zeng, L., Wu, T., Zhao, H., Huang, Y., Bedzyk, M.J., Sritharan, T.: Valence change ability and geometrical occupation of substitution cations determine the pseudocapacitance of spinel ferrite XFe_2O_4 (X = Mn, Co, Ni, Fe). Chem. Mater. **28**, 4129–4133 (2016)
13. Shisode, M., Kharat, P.B., Bhoyar, D.N., Vinayak, V., Babrekar, M., Jadhav, K.: Structural and multiferroic properties of Ba2+ doped $BiFeO_3$ nanoparticles synthesized via sol-gel method. In: AIP Conference Proceedings, p. 030276. AIP Publishing (2018)
14. Humbe, A.V., Kharat, P.B., Nawle, A.C., Jadhav, K.: Nanocrystalline $Ni_{0.70-x}Cu_xZn_{0.30}Fe_2O_4$ with $0 \leq x \leq 0.25$ prepared by nitrate-citrate route: structure, morphology and electrical investigations. J. Mater. Sci. Mater. Electron. **29**, 3467–3481 (2018)
15. Kale, G., Humbe, A.V., Kharat, P., Bhoyar, D., Jadhav, K.: Tartaric acid a novel fuel approach: synthesis and characterization of $CoFe_2O_4$ nanoparticles. Bionano Frontier **8**, 146–148 (2015)
16. Ghadikolaei, S., Yassari, M., Sadeghi, H., Hosseinzadeh, K., Ganji, D.: Investigation on thermophysical properties of TiO_2–Cu/H_2O hybrid nanofluid transport dependent on shape factor in MHD stagnation point flow. Powder Technol. **322**, 428–438 (2017)
17. Malvandi, A., Moshizi, S., Ganji, D.: Nanoparticle transport effect on magnetohydrodynamic mixed convection of electrically conductive nanofluids in micro-annuli with temperature-dependent thermophysical properties. Phys. E: Low-Dimens. Syst. Nanostruct. **88**, 35–49 (2017)
18. Gupta, M., Singh, V., Kumar, R., Said, Z.: A review on thermophysical properties of nanofluids and heat transfer applications. Renew. Sustain. Energy Rev. **74**, 638–670 (2017)
19. Afrand, M.: Experimental study on thermal conductivity of ethylene glycol containing hybrid nano-additives and development of a new correlation. Appl. Therm. Eng. **110**, 1111–1119 (2017)
20. Ganesan, V., Louis, C., Damodaran, S.P.: Novel nanofluids based on magnetite nanoclusters and investigation on their cluster size-dependent thermal conductivity. J. Phys. Chem. C **122**, 6918–6929 (2018)
21. Hajmohammadi, M.: Cylindrical Couette flow and heat transfer properties of nanofluids; single-phase and two-phase analyses. J. Mol. Liq. **240**, 45–55 (2017)
22. Karimi, A., Afghahi, S.S.S., Shariatmadar, H., Ashjaee, M.: Experimental investigation on thermal conductivity of MFe_2O_4 (M = Fe and Co) magnetic nanofluids under influence of magnetic field. Thermochim. Acta **598**, 59–67 (2014)
23. Karimi, A., Sadatlu, M.A.A., Saberi, B., Shariatmadar, H., Ashjaee, M.: Experimental investigation on thermal conductivity of water based nickel ferrite nanofluids. Adv. Powder Technol. **26**, 1529–1536 (2015)
24. Amani, M., Amani, P., Kasaeian, A., Mahian, O., Wongwises, S.: Thermal conductivity measurement of spinel-type ferrite $MnFe_2O_4$ nanofluids in the presence of a uniform magnetic field. J. Mol. Liq. **230**, 121–128 (2017)
25. Shahsavar, A., Salimpour, M.R., Saghafian, M., Shafii, M.: Effect of magnetic field on thermal conductivity and viscosity of a magnetic nanofluid loaded with carbon nanotubes. J. Mech. Sci. Technol. **30**, 809–815 (2016)
26. Kharat, P.B., Kounsalye, J.S., Shisode, M.V., Jadhav, K.: Preparation and thermophysical investigations of $CoFe_2O_4$-based nanofluid: a potential heat transfer agent. J. Supercond. Nov. Magn. 1–11. https://doi.org/10.1007/s10948-018-4711-y (2018)
27. Kharat, P.B., Somvanshi, S.B., Kounsalye, J.S., Deshmukh, S.S., Khirade, P.P., Jadhav, K.: Temperature dependent viscosity of cobalt ferrite/ethylene glycol ferrofluids. In: AIP Conference Proceedings, p. 050044. AIP Publishing (2018)
28. Din, I.U., Tasleem, S., Naeem, A., Shaharun, M.S., Nasir, Q.: Study of annealing conditions on particle size of nickel ferrite nanoparticles synthesized by wet chemical route. Synth. React. Inorg., Met.-Org., Nano-Met. Chem. **46**, 405–408 (2016)
29. Dolla, T.H., Pruessner, K., Billing, D.G., Sheppard, C., Prinsloo, A., Carleschi, E., Doyle, B., Ndungu, P.: Sol-gel synthesis of $Mn_xNi_{1-x}Co_2O_4$ spinel phase materials: structural, electronic, and magnetic properties. J. Alloys Compd. **742**, 78–89 (2018)

30. Kharat, P.B., JSK, A.V.H., Birajdar, S.D., Jadhav, K.: Preparation and diverse properties of cobalt ferrite ferrofluid. Int. J. Adv. Res. Basic Appl. Sci. (2), 106–109 (2017)
31. Kounsalye, J.S., Kharat, P.B., Chavan, A.R., Humbe, A.V., Borade, R., Jadhav, K.: Symmetry transition via tetravalent impurity and investigations on magnetic properties of $Li_{0.5}Fe_{2.5}O_4$. In: AIP Conference Proceedings, p. 050067. AIP Publishing (2018)
32. Kounsalye, J.S., Kharat, P.B., Bhoyar, D.N., Jadhav, K.: Radiation-induced modifications in structural, electrical and dielectric properties of Ti4+ ions substituted $Li_{0.5}Fe_{2.5}O_4$ nanoparticles. J. Mater. Sci. Mater. Electron. **29**, 8601–8609 (2018)
33. Wang, Y., Li, L., Zhang, Y., Chen, X., Fang, S., Li, G.: Growth kinetics, cation occupancy, and magnetic properties of multimetal oxide nanoparticles: a case study on spinel $NiFe_2O_4$. J. Phys. Chem. C **121**, 19467–19477 (2017)
34. Yadav, R.S., Kuřitka, I., Vilcakova, J., Havlica, J., Masilko, J., Kalina, L., Tkacz, J., Enev, V., Hajdúchová, M.: Structural, magnetic, dielectric, and electrical properties of $NiFe_2O_4$ spinel ferrite nanoparticles prepared by honey-mediated sol-gel combustion. J. Phys. Chem. Solids **107**, 150–161 (2017)
35. Reddy, M.P., Shakoor, R., Mohamed, A.: Auto combustion synthesis, microstructural and magnetic characteristics of nickel ferrite nanoparticles. Indian J. Sci. Technol. **10**(13). https://doi.org/10.17485/ijst/2017/v10i13/88034 (2017)
36. Aghazadeh, M., Karimzadeh, I., Ganjali, M.R.: Ethylenediaminetetraacetic acid capped superparamagnetic iron oxide (Fe_3O_4) nanoparticles: a novel preparation method and characterization. J. Magn. Magn. Mater. **439**, 312–319 (2017)
37. Manikandan, V., Li, X., Mane, R., Chandrasekaran, J.: Room temperature gas sensing properties of Sn-substituted nickel ferrite ($NiFe_2O_4$) thin film sensors prepared by chemical co-precipitation method. J. Electron. Mater. 1–6 (2018)
38. Ramirez, S., Chan, K., Hernandez, R., Recinos, E., Hernandez, E., Salgado, R., Khitun, A., Garay, J., Balandin, A.: Thermal and magnetic properties of nanostructured densified ferrimagnetic composites with graphene-graphite fillers. Mater. Des. **118**, 75–80 (2017)
39. Corner, W., Tanner, B.: Magnetic domains. Phys. Educ. **11**, 356 (1976)
40. Hubert, A., Schäfer, R.: Magnetic domains: the analysis of magnetic microstructures. Springer Science & Business Media (2008)
41. Gromova, Y.A., Maslov, V.G., Baranov, M.A., Serrano-García, R., Kuznetsova, V.A., Purcell-Milton, F., Gun'ko, Y.K., Baranov, A.V., Fedorov, A.V.: Magnetic and optical properties of isolated and aggregated $CoFe_2O_4$ superparamagnetic nanoparticles studied by MCD spectroscopy. J. Phys. Chem. C **122**, 11491–11497 (2018)
42. Carey, V.P.: Liquid Vapor Phase Change Phenomena: an Introduction to the Thermophysics of Vaporization and Condensation Processes in Heat Transfer Equipment. CRC Press, Boca Raton (2018)
43. Yadav, R.: Synthesis and characterization of structural and magnetic properties of electrodeposited cobalt iron thin film. Indian Institute of Technology Hyderabad (2015)
44. Asadi, A., Asadi, M., Rezaniakolaei, A., Rosendahl, L.A., Afrand, M., Wongwises, S.: Heat transfer efficiency of Al_2O_3-MWCNT/thermal oil hybrid nanofluid as a cooling fluid in thermal and energy management applications: an experimental and theoretical investigation. Int. J. Heat Mass Transf. **117**, 474–486 (2018)
45. De Sciarra, F.M., Russo, P.: Experimental Characterization, Predictive Mechanical and Thermal Modeling of Nanostructures and Their Polymer Composites. William Andrew, New York (2018)
46. Cao, G.: Nanostructures & Nanomaterials: Synthesis, Properties & Applications. Imperial College Press, London (2004)
47. Priyananda, P., Sabouri, H., Jain, N., Hawkett, B.S.: Steric stabilization of γ-Fe_2O_3 superparamagnetic nanoparticles in a hydrophobic ionic liquid and the magnetorheological behavior of the ferrofluid. Langmuir **34**, 3068–3075 (2018)
48. Ma, B., Banerjee, D.: A review of nanofluid synthesis. In: Advances in Nanomaterials, pp. 135–176. Springer, Berlin (2018)
49. Kharat, P.B., Shisode, M., Birajdar, S., Bhoyar, D., Jadhav, K.: Synthesis and characterization of water based $NiFe_2O_4$ ferrofluid. In: AIP Conference Proceedings, p. 050122. AIP Publishing (2017)
50. Li, C., Strachan, A.: Cohesive energy density and solubility parameter evolution during the curing of thermoset. Polymer **135**, 162–170 (2018)